Supplementary Information

Creation and characterization of warm dense matter isochorically heated by an intense laser-driven proton beam to temperatures exceeding 100 eV

M. Bailly-Grandvaux[1,*], S. Bolaños[1], J. Kim[1], J. Saret[1], C. McGuffey[2], K. Bhutwala[1], P. Nilson[3], T. Filkins[3], W. Theobald[3], A. Haid[2], S. Ivancic[3], and F.N. Beg[1]

[1]Center for Energy Research, University of California, San Diego, San Diego, CA
[2]General Atomics, San Diego, CA
[3]Laboratory for Laser Energetics, Rochester, NY
[*]mbaillyg@ucsd.edu

Initialization of ion heating simulations with the radiation-hydrodynamics code HELIOS

The on-target power density, $I(t)$, of an ion beam with a typical Maxwell-Boltzmann energy distribution, characterized by a total energy W and a temperature T, generated at a source-to-target distance d, and having a Full-Width-Half-Maximum (FWHM) beam size on target, ϕ_{FWHM}, can be analytically derived as follows[1]:

$$I(t) = \frac{8}{3\sqrt{\pi}} \frac{\left(\frac{W}{\tau}\right)\left(\frac{\tau}{t}\right)^6 \exp\left(-\tau/t\right)^2}{\pi\phi_{\mathrm{FWHM}}^2/4},$$

where $\tau = d/\sqrt{2T/m_i}$ with m_i the mass of the ion

The quantities W and T are here determined from experimental measurements using a stack of radiochromic films (RCF) and a Thomson parabola (TPIE) spectrometer. The distance d is known from the experimental geometry. The remaining free parameter ϕ_{FWHM} for protons is here supported by the Bayesian analysis of the measured K_α spectra and further corroborated by 2D LSP simulations, which model proton focusing and transport within the cone-enclosed hemisphere. Regardless of these considerations, the time evolution of a normalized ion current $I(t)$ for a specific ion species is solely determined by the value of τ and can thus be fully described with minimal assumptions.

By combining $I(t)$ with a time-of-flight table for ion kinetic energy $E_k(t)$, the ion energy flux can be used as an energy source input for radiation-hydrodynamics simulations. To complete this process, the energy deposition for a given E_k and ion species must be calculated using a stopping-power model. The 1D radiation-hydrodynamics code HELIOS[2] provides this functionality by allowing the user to input the two tables, $I(t)$ and $E_k(t)$, and uses the Mehlhorn model to calculate stopping-power in plasmas for the chosen ion[3].

Results from the heating simulations

The input parameters for the proton beam are as follows: $W = 15$ J, $T = 5$ MeV, and $\phi_{\mathrm{FWHM}} = 50$ µm. The values of W and T are directly obtained from RCF and TPIE measurements, while ϕ_{FWHM} is inferred from the Bayesian analysis and 2D LSP simulations. The input parameters for the carbon beam are: $W = 4.2$ J, $T = 14$ MeV, and $\phi_{\mathrm{FWHM}} = 150$ µm. The value of T for the carbon beam is directly obtained from the TPIE measurement of the C^{6+} trace, which represents the dominant charge state of the carbon ions (see Fig. 8 in the main text). The value of W is estimated by calculating the ratio of total energy between the C^{6+} and proton spectra recorded by the TPIE diagnostic. It is further assumed that carbon ions have the same angular distribution as protons, allowing for an extrapolation to the full beam energy. Additionally, we assume that ϕ_{FWHM} for the carbon beam is equal to the cone-tip diameter, as the cone focusing fields are likely less effective in further focusing carbon ions due to their lower charge-to-mass ratio compared to protons. It is important to note that the validity of these assumptions does not affect the timing of the heating, which is fully determined by the value of τ. This timing is well constrained by the measurements of T and the geometry, with $d = 430$ µm.

In Figure 1, we present the results of 1D HELIOS radiation-hydrodynamics simulations showing the heating induced by the proton beam (first row) and the carbon ion beam (second row) in solid-density copper targets. These targets have thicknesses of either 10 µm (first column) or 25 µm (second column). The temperature distribution in the proton-heated targets is notably uniform throughout the depth of the targets. In contrast, the heating by the carbon ions is concentrated within the first ~ 4 µm

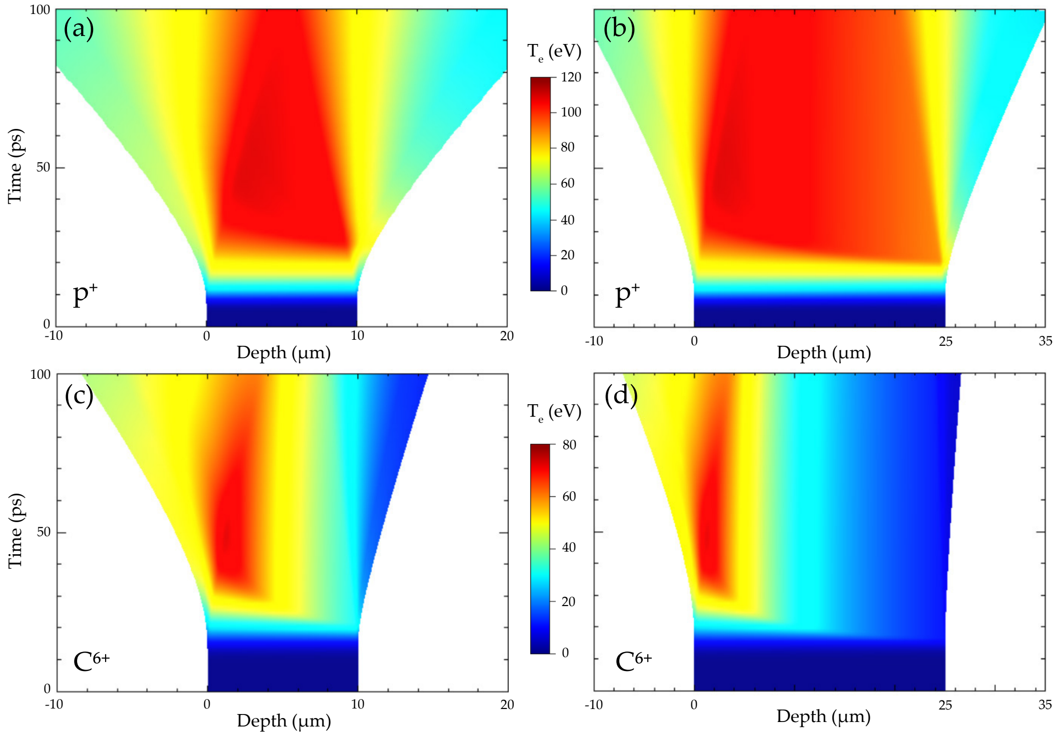

Figure 1. HELIOS radiation-hydrodynamic simulations of proton beam (first row) and carbon ion beam (second row) heating in 10 μm-thick (first column) or 25 μm-thick (second column) solid density copper.

of the target. Additionally, the carbon ion heating is delayed by approximately 10 ps compared to the protons. The main heating occurs at around 30 ps for the carbon ions, whereas it starts at approximately 20 ps for the protons. As a result, we expect a longitudinal temperature gradient to develop for times $t > 30$ ps.

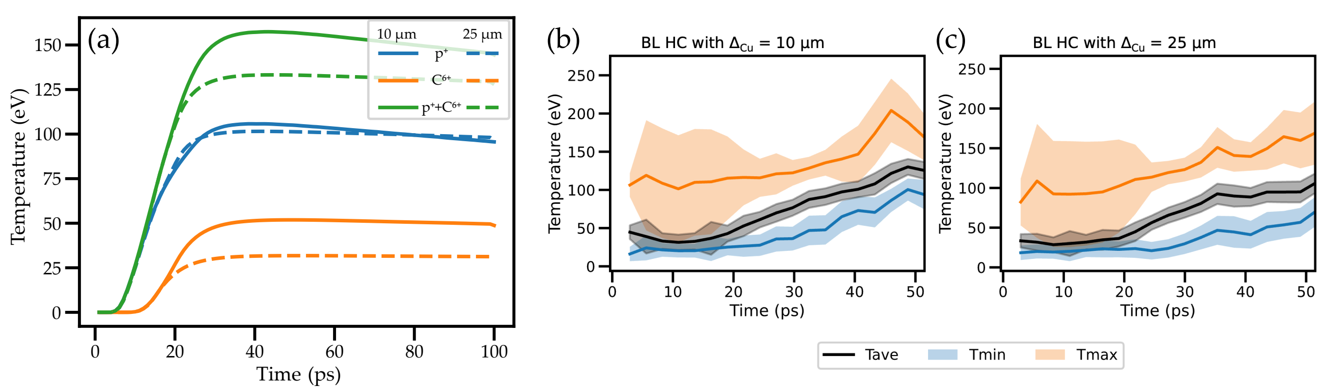

Figure 2. (a) Temperature averaged within the depth of the 10 μm-thick (solid lines) and 25 μm-thick (dashed lines) solid density copper targets, extracted from HELIOS simulations for the proton beam (blue lines), carbon ion beam (orange lines) and the sum of proton and carbon ions (green lines). Temperature evolution estimated from a Bayesian analysis of the experimental K_α spectra for HC targets in the BL configuration for the 10 μm-thick (b) and 25 μm-thick (c) copper samples. The orange line represents $T_{\max}$, the blue line represents $T_{\min}$, and the black line indicates the radial average temperature.

The temperature averaged over the depth of the copper targets from the HELIOS simulations is shown in Figure 2-(a). Results for the 10 μm-thick and 25 μm-thick targets are depicted by solid and dashed lines, respectively. The simulated average temperatures due to energy deposition from the proton beam, carbon ion beam, and the combined proton and carbon ion beams are represented by blue, orange, and green lines, respectively. We can again observe the uniform longitudinal temperature distribution from the proton beams, with nearly identical temperatures for both the 10 μm and 25 μm thick targets. In contrast, the carbon ion beam shows greater variation between the two target thicknesses, as its energy is primarily deposited near the front of the target. The delay in carbon ion heating, by approximately 10 ps compared to protons, is also evident in the evolution of these average temperatures. As a result of the non-uniform energy deposition by the carbon ions, the simulations predict a lower average temperature for the 25 µm-thick target compared to the 10 µm-thick target. Additionally, we expect the minimum temperature to be lower for the 25 µm-thick target, while the maximum temperatures for both targets are expected to be similar.

In Figure 2-(b-c), we present the results of the Bayesian analysis of the experimental K_α spectra for HC targets in the BL configuration, corresponding to the 10 µm (b) and 25 µm (c) thick targets, respectively. Consistent with the HELIOS simulation predictions, we observe a slightly lower average temperature for the 25 µm target, similar maximum temperatures, and a noticeably lower minimum temperature. It is important to note that, as expected, the 1D simulations tend to overestimate the temperature. However, the relative trends and heating dynamics are convincingly reproduced. These results support the discussion in the main paper regarding the role of heavier ions during the late-time heating phase, specifically the development of a longitudinal gradient localized near the target's front surface, which contributes to an increase in the inferred values of maximum temperature and FWHM.

References

1. Temporal, M., Honrubia, J. J. & Atzeni, S. Numerical study of fast ignition of ablatively imploded deuterium-tritium fusion capsules by ultra-intense proton beams. *Phys. Plasmas* **9**, 3098–3107, DOI: 10.1063/1.1482375 (2002).

2. Macfarlane, J. J., Golovkin, I. E. & Woodruff, P. R. HELIOS-CR - A 1-D radiation-magnetohydrodynamics code with inline atomic kinetics modeling. *J. Quant. Spectrosc. Radiat. Transf.* **99**, 381–397, DOI: 10.1016/j.jqsrt.2005.05.031 (2006).

3. Mehlhorn, T. A. A finite material temperature model for ion energy deposition in ion-driven inertial confinement fusion targets. *J. Appl. Phys.* **52**, 6522–6532, DOI: 10.1063/1.328602 (1981).